Spectrochimica Acta Part A 84 (2011) 184–195

Contents lists available at SciVerse ScienceDirect

Spectrochimica Acta Part A: Molecular and Biomolecular Spectroscopy

journal homepage: www.elsevier.com/locate/saa

Molecular structure, vibrational spectroscopic, first-order hyperpolarizability and HOMO, LUMO studies of 2-aminobenzimidazole

S. Sudha[a], M. Karabacak[b], M. Kurt[c], M. Cinar[b], N. Sundaraganesan[a,*]

[a] Department of Physics (Engg.), Annamalai University, Annamalai Nagar 608 002, Chidambaram, Tamil Nadu, India
[b] Department of Physics, Afyon Kocatepe University, Afyonkarahisar 03040, Turkey
[c] Department of Physics, Ahi Evran University, Kırşehir 40100, Turkey

ARTICLE INFO

Article history:
Received 25 July 2011
Received in revised form 5 September 2011
Accepted 7 September 2011

Keywords:
FTIR
FT-Raman
TD-DFT
TED
HOMO–LUMO
2-Aminobenzimidazole

ABSTRACT

In the present work, we reported a combined experimental and theoretical study on molecular structure, vibrational spectra and HOMO–LUMO analysis of 2-aminobenzimidazole (2-ABD). The FTIR (400–4000 cm^{-1}) and FT-Raman spectra (50–3500 cm^{-1}) of 2-ABD were recorded. The molecular geometry, harmonic vibrational wavenumbers and bonding features of 2-ABD in the ground-state have been calculated by using the density functional B3LYP method with 6-311++G(d,p) and 6-31G(d) as basis sets. The energy and oscillator strength were calculated by time-dependent density functional theory (TD-DFT) result complements with the experimental findings. The calculated HOMO and LUMO energies showed that charge transfer occurs within the molecule. Finally, the calculation results were applied to simulate infrared and Raman spectra of the title compound which showed good agreement with the observed spectra.

1. Introduction

There are 30 derivatives of 2-aminobenzimidazole registered in the world as drugs, which exhibit diverse pharmacological activities, e.g. antiparasitic, antifungal, antiviral and antiallergic [1]. The 2-aminobenzimidazoles are promising class of chemical compounds with different biological effects as immunotropic, diuretic, antihistaminic as well as highly selective p38a MAP inhibition properties [2–6]. The polyfunctionality of the 2-aminobenzimidazole molecule resulting from the cyclic guanidine moiety has made it a building block for the synthesis of a large number of benzimidazole derivatives of pharmacological interest. The 2-aminobenzimidazole derivatives active against herpes simplex virus (HSV), human cyclomegalo virus (HCMV) and HIV were also described and patented [7–11]. A group of complex compounds of 2-aminobenzimidazole derivatives with some metals, such as cobalt, zinc and copper, showed also antifungal and antibacterial activity [12–14], while complexes with ruthenium [15] were cytotoxic in vitro against SKW-8 cells (human T-lymphoma). 2-Aminobenzimidazole is the core of a number of bioactive benzimidazole derivatives. This benzimidazole moiety is also a substructure of chemosensor receptors used for selective recognition of anions with an important role in a variety of biological activities.

Until now, the energies of the singlet-excited states of 2-aminobenzimidazole with aromatic ketones were calculated using the time-dependent (TD-DFT) method and electronic structures of stationary points were analyzed by the natural bond orbital (NBO) method. HOMO and LUMO energy gap were also calculated by using B3LYP/6-31G* method [16]. Solid state linear dichroic IR spectral analysis of 2-aminobenzimidazole and its N_1-protonated salts has been investigated by Ivanova [17]. Recently, Sundaraganesan et al. [18] have been investigated the vibrational spectra and DFT studies of benzimidazole. Güllüoglu et al. [19,20] have been studied the molecular structure and vibrational spectra of 2- and 5-methylbenzimidazole and 4-phenylimidazole. Most recently, Angelova et al. carried out an investigation of 2-aminobenzimidazole by UV and IR spectroscopy along with theoretical calculations at HF, MP2 and DFT levels [21].

The combination of vibrational spectroscopy coupled with quantum mechanical calculations can be a powerful method for understanding the structural, conformational, vibrational and electronic behavior of molecules. Electronic correlation to the calculations is necessary to get more reliable results on the structural parameters, physio-chemical properties and vibrational properties [22,23]. Harmonic force fields of polyatomic molecules play a vital role in the interpretation of vibrational spectra and in the prediction of vibrational properties. Now-a-days the anharmonic wavenumbers also can be calculated which give better description

* Corresponding author. Tel.: +91 9442068405.
E-mail address: sundaraganesan_n2003@yahoo.co.in (N. Sundaraganesan).

1386-1425/$ – see front matter © 2011 Elsevier B.V. All rights reserved.
doi:10.1016/j.saa.2011.09.028

Table 1a
The calculated all β components and β_{tot} ($\times 10^{-33}$) value of 2-aminobenzimidazole.

	B3LYP/6-311++G(d,p)			B3LYP/6-311++G(d,p)	
	(a.u.)	esu ($\times 10^{-24}$)		(a.u.)	esu ($\times 10^{-33}$)
α_{xx}	152.99756	22.67424	β_{xxx}	453.73998	3919.9958
α_{xy}	−1.35478	−0.20078	β_{xxy}	−34.234349	−295.76081
α_{yy}	58.92297	8.73238	β_{xyy}	60.190354	520.00253
α_{xz}	0.35303	0.05232	β_{yyy}	−8.813189	−76.139784
α_{yz}	3.60092	0.53366	β_{xxz}	−35.456735	−306.32137
α_{zz}	104.30124	15.45744	β_{xyz}	−1.8477878	−15.963593
α_{tot}	105.40726	15.62136	β_{yyz}	−5.8699909	−50.712612
$\Delta\alpha$	81.76217	12.11715	β_{xzz}	5.568984	48.112123
			β_{yzz}	2.6952509	23.285081
			β_{zzz}	5.0891991	43.967118
			β_{tot}	522.3227	4512.5025

Table 1b
The calculated electric dipole moments m (D) and dipole moment components for 2-aminobenzimidazole.

	B3LYP/6-311++G(d,p)
μ_x	−0.9220227
μ_y	−0.3736421
μ_z	−1.1519933
μ	1.52211131

of the molecular properties. In our present investigation, owing to the pharmacological activities and biological effects of 2-ABD, the FTIR and FT-Raman vibrational wavenumbers are determined and by using quantum chemical calculations, the wavenumbers were theoretically calculated. Many organic molecules, containing conjugated π electrons and characterized by large values of molecular first hyperpolarizabilities, were analyzed by means of vibrational spectroscopy [24]. In this context, the hyperpolarizability of the title compound is also calculated in the present work.

2. Experimental

The 2-aminobenzimidazole sample was purchased from Sigma–Aldrich Chemical Company (USA) with a stated purity of 97% and it was used as such without further purification. The sample was prepared using a KBr disc technique because of solid state. The IR spectrum of molecule was recorded in the region of 400–4000 cm^{-1} on a Perkin Elmer FTIR BX spectrometer calibrated using polystyrene bands. FT-Raman spectrum of the sample was recorded using 1064 nm line of Nd:YAG laser as excitation wave length in the region of 50–4000 cm^{-1} on a Bruker RFS 100/S FT-Raman. The detector is a liquid nitrogen cooled Ge detector. Five hundred scans were accumulated at 4 cm^{-1} resolution using a laser power of 100 mW. The UV–Vis absorption spectrum of the sample was examined in the range of 200–400 nm using Shimadzu UV-1800 PC, UV-Vis recording Spectrophotometer in ethanol solution and water.

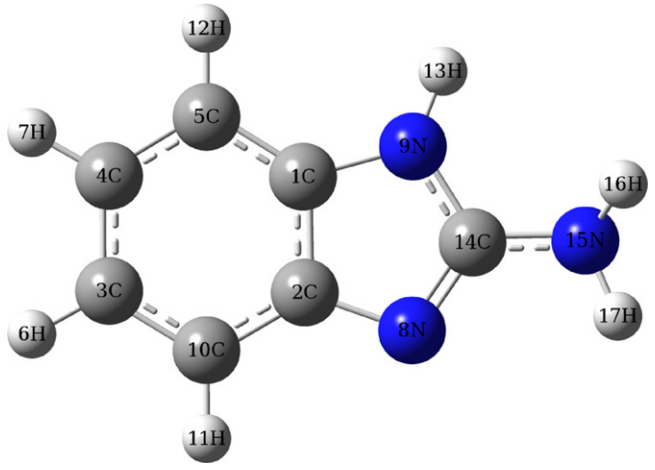

Fig. 1. Molecular structure with atom numbering scheme of 2-aminobenzimidazole.

3. Computational details

The combination of spectroscopic methods with DFT calculations are powerful tools for understanding the fundamental vibrational properties and the electronic structure of the compounds. To provide complete information regarding to the structural characteristics and the fundamental vibrational modes of 2-aminobenzimidazole, the DFT-B3LYP correlation functional calculations have been carried out. The calculations of geometrical parameters in the ground state were performed using the Gaussian 03 [25] program. DFT calculations were carried out with Becke's three-parameter hybrid model using the Lee–Yang–Parr correlation functional (B3LYP) method. The geometry optimization was carried out using the initial geometry generated from standard geometrical parameters at B3LYP method by adopting split-valence polarized 6-311++G(d,p) basis set. The optimum geometry was determined by minimizing the energy with respect to all geometrical parameters without imposing molecular symmetry constraints. Harmonic vibrational wavenumbers were calculated using analytic second derivatives to confirm the convergence to minima in the potential surface. At the optimized structure of the examined species, no imaginary wavenumber modes were obtained, proving that a true minimum on the potential surface was found. The IR intensities were calculated from the dipole moment derivatives with respect to normal coordinates, while polarizability derivatives for Raman activities were obtained using numerical differentiation of the analytical dipole moment derivatives with respect to the applied electric field. The relative intensity of the most intense line appears to be theoretically overestimated by comparison with experimental IR and Raman bands. The vibrational modes were assigned on the basis of TED analysis using VEDA 4 program [26]. The total energy distribution corresponding to each of the observed wavenumbers shows the reliability and accuracy of the spectral analysis. The electronic properties such as HOMO and LUMO energies were determined by time-dependent DFT (TD-DFT) approach, while taking solvent effect into account.

4. Prediction of Raman intensity and first order hyperpolarizability

The Raman activities (S_{Ra}) calculated with Gaussian 03 program [25] converted to relative Raman intensities (I_{Ra}) using the

following relationship derived from the intensity theory of Raman scattering [27,28]

$$I_i = \frac{f(\nu_0 - \nu_i)^4 S_i}{\nu_i[1 - \exp(-hc\nu_i/kT)]}$$

where ν_0 is the laser exciting wavenumber in cm^{-1} (in this work, we have used the excitation wavenumber $\nu_0 = 9398.5\ cm^{-1}$, which corresponds to the wavelength of 1064 nm of a Nd:YAG laser), ν_i is the vibrational wavenumber of the ith normal mode (cm^{-1}), while S_i is the Raman scattering activity of the normal mode ν_i. f (is a constant equal to 10^{-12}) is a suitably chosen common normalization factor for all peak intensities. h, k, c and T are Planck and Boltzmann constants, speed of light and temperature in Kelvin, respectively.

The first hyperpolarizability (β_0) of this novel molecular system, and related properties (β, α_0 and $\Delta\alpha$) of 2-ABD are calculated using B3LYP/6-311++G(d,p) method, based on the finite-field approach. In the presence of an applied electric field, the energy of a system is a function of the electric field. First hyperpolarizability is a third rank tensor that can be described by $3 \times 3 \times 3$ matrices. The 27 components of the 3D matrix can be reduced to 10 components due to the Kleinman symmetry [29]. It can be given in the lower tetrahedral format. It is obvious that the lower part of the $3 \times 3 \times 3$ matrices is a tetrahedral. The components of β are defined as the coefficients in the Taylor series expansion of the energy in the external electric field. When the external electric field is weak and homogeneous, this expansion becomes:

$$E = E^0 - \mu_\alpha F_\alpha - \frac{1}{2}\alpha_{\alpha\beta}F_\alpha F_\beta - \frac{1}{6}\beta_{\alpha\beta\gamma}F_\alpha F_\beta F_\gamma + \cdots$$

where E^0 is the energy of the unperturbed molecules, F_α is the field at the origin, μ_α, $\alpha_{\alpha\beta}$ and $\beta_{\alpha\beta\gamma}$ are the components of dipole moment, polarizability and the first hyperpolarizabilities, respectively. The total static dipole moment μ, the mean polarizability α_0, the anisotropy of the polarizability $\Delta\alpha$ and the mean first hyperpolarizability β_0, using the x, y, z components they are defined as:

$$\mu = (\mu_x^2 + \mu_y^2 + \mu_z^2)^{1/2}$$

$$\alpha_0 = \frac{\alpha_{xx} + \alpha_{yy} + \alpha_{zz}}{3}$$

$$\alpha = 2^{-1/2}[(\alpha_{xx} - \alpha_{yy})^2 + (\alpha_{yy} - \alpha_{zz})^2 + (\alpha_{zz} - \alpha_{xx})^2 + 6\alpha_{xx}^2]^{1/2}$$

$$\beta_0 = (\beta_x^2 + \beta_y^2 + \beta_z^2)^{1/2}$$

and

$$\beta_x = \beta_{xxx} + \beta_{xyy} + \beta_{xzz}$$

$$\beta_y = \beta_{yyy} + \beta_{xxy} + \beta_{yzz}$$

$$\beta_z = \beta_{zzz} + \beta_{xxz} + \beta_{yyz}$$

Since the values of the polarizabilities (α) and hyperpolarizability (β) of the Gaussian 03 output are reported in atomic units (a.u.), the calculated values have been converted into electrostatic units (esu) (α: 1 a.u. = 0.1482×10^{-24} esu; β: 1 a.u. = 8.639×10^{-33} esu).

The total molecular dipole moment and first order hyperpolarizability are 1.5221 D and 4.5125×10^{-30} esu, respectively and are depicted in Tables 1a and 1b. Total dipole moment of title molecule is approximately equal to those of urea and first hyperpolarizability of title molecule is 12 times greater than those of urea (μ and β of urea are 1.3732 D and 0.3728×10^{-30} esu obtained by HF/6-311G(d,p) method).

Table 2
The calculated geometric parameters of 2-aminobenzimidazole, bond lengths in angstrom (Å) and angles in degrees (°).

Parameters	B3LYP/6-311++G(d,p)	B3LYP/6-31G(d)	X-Ray Benzimidazole[a]
Bond length			
C1–C2	1.413	1.416	1.392
C1–C5	1.389	1.391	1.401
C1–N9	1.394	1.394	1.395
C2–N8	1.392	1.393	1.372
C2–C10	1.395	1.397	1.389
C3–C4	1.403	1.405	1.401
C3–H6	1.084	1.087	1.020
C3–C10	1.394	1.395	1.378
C4–C5	1.396	1.397	1.386
C4–H7	1.084	1.086	1.070
C5–H12	1.084	1.087	0.980
N8–C14	1.306	1.310	1.311
N9–H13	1.007	1.009	0.900
N9–C14	1.381	1.382	1.346
C10–H11	1.083	1.086	0.940
C14–N15	1.382	1.386	
N15–H16	1.011	1.015	
N15–H17	1.011	1.014	
Bond angles			
C2–C1–C5	122.7	122.8	122.4
C2–C1–N9	104.5	104.5	105.8
C5–C1–N9	132.7	132.7	
C1–C2–N8	110.4	110.6	109.5
C1–C2–C10	119.6	119.5	120.6
N8–C2–C10	130.0	129.9	
C4–C3–H6	119.1	119.2	
C4–C3–C10	121.5	121.4	120.9
H6–C3–C10	119.4	119.4	117.0
C3–C4–C5	121.2	121.3	122.3
C3–C4–H7	119.5	119.5	111.0
C5–C4–H7	119.3	119.2	
C1–C5–C4	116.8	116.8	116.1
C1–C5–H12	122.0	122.0	
C4–C5–H12	121.1	121.2	121.0
C2–N8–C14	105.0	104.6	104.2
C1–N9–H13	126.3	126.2	121.0
C1–N9–C14	106.5	106.4	106.6
H13–N9–C14	125.6	125.3	
C2–C10–C3	118.1	118.2	117.8
C2–C10–H11	120.3	120.2	117.0
C3–C10–H11	121.5	121.6	114.0
N8–C14–N9	113.6	113.9	
N8–C14–N15	125.4	125.4	
N9–C14–N15	120.9	120.7	
C14–N15–H16	115.8	114.6	
C14–N15–H17	111.8	110.5	
H16–N15–H17	112.3	111.1	
Dihedral angles			
C5–C1–C2–N8	−179.6	−179.6	
N9–C1–C2–C10	179.2	179.0	
C5–C1–N9–C14	−179.7	−179.6	
C10–C2–N8–C14	179.9	179.9	
C1–N9–C14–N8	−1.7	−2.0	
C1–N9–C14–N15	175.6	175.4	
N8–C14–N15–H16	−140.1	−135.7	
N8–C14–N15–H17	−9.8	−9.3	
N9–C14–N15–H16	43.0	47.1	
N9–C14–N15–H17	173.3	173.5	

[a] Taken from Ref. [28].

5. Results and discussion

5.1. Molecular structure

The optimized geometrical parameters of 2-aminobenzimidazole derived from the structure refinement, as well as those obtained from quantum chemical calculations are listed in Table 2, which are in accordance with the atom numbering scheme given in Fig. 1. Our optimized structural

parameters are compared with the XRD data of closely related molecule benzimidazole [30]. The calculated geometrical parameters represent a good approximation and they are the bases for the calculating other parameters, such as vibrational wavenumbers and electronic properties. From the structural data shown in Table 2, it is illustrated that some of the bond lengths and bond angles are found to be greater than the experimental data. This overestimation can be explained that the theoretical calculations belong to isolated molecule in gaseous phase and the experimental results belong to similar molecule in solid state. The molecular structure is almost planar as it is evident from the bond and dihedral angle values given in Table 2. But the amino group substituted in the 2nd position shows that it is out-of-plane as it is evident from the torsional angles of N8–C14–N15–H17 = −9.8° and N9–C14–N15–H16 = 43.0°. Many researchers [31,32] have explained the changes in the frequency or bond length of C–H bond on substitution due to a change in the charge distribution on the carbon atom of the benzene ring. In substituted benzenes, the ring carbon atoms exert a large attraction on the valence electron cloud of the H atom resulting in an increase in the C–H force constant and a decrease in the corresponding bond length. The C14=N8 bond length is shorter than the other C–N bond lengths and also a noticeable difference between the calculated and experimental data is observed, it may be due to the presence of intermolecular hydrogen bonding [33].

The experimental C–C bond lengths fall in the range of 1.378–1.401 Å and the optimized C–C bond lengths in 2-ABD fall in the ranges of 1.389–1.413 Å and 1.391–1.416 Å by B3LYP/6-311++G(d,p) and B3LYP/6-31G(d) methods, respectively. The calculated C–C bond lengths are in excellent agreement with the

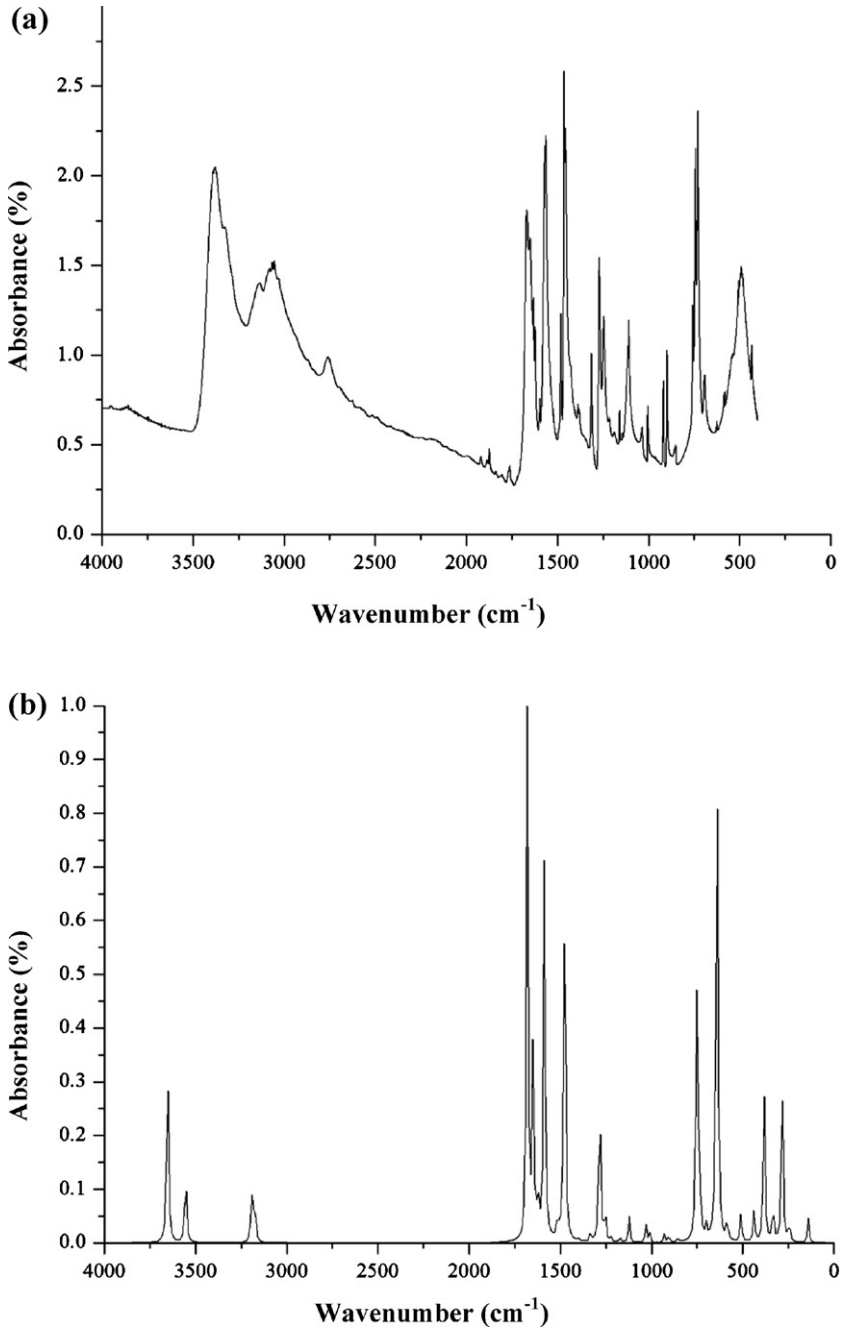

Fig. 2. Experimental (a) and theoretical (b) IR spectra of 2-aminobenzimidazole.

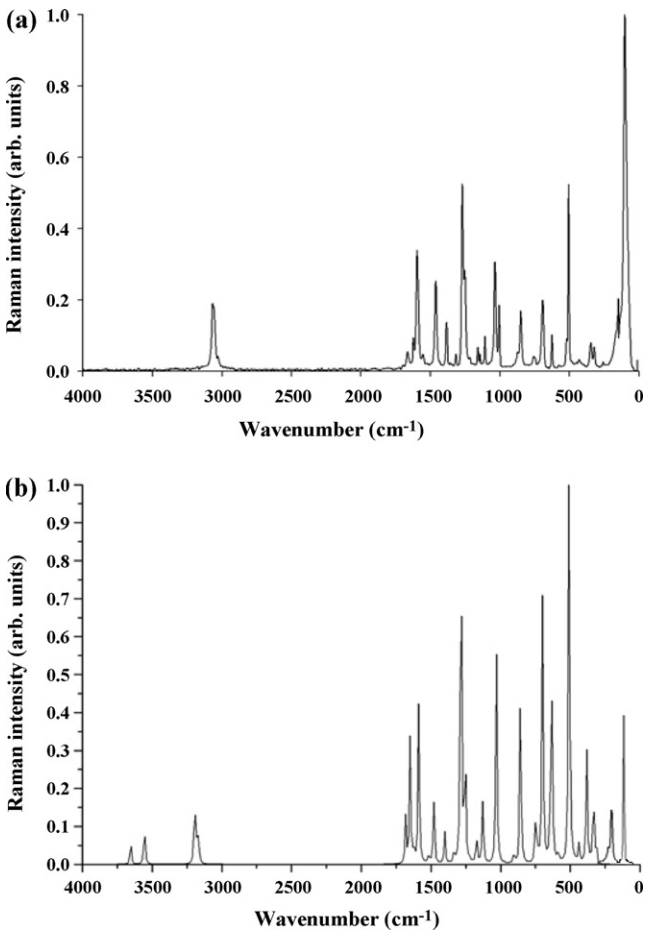

Fig. 3. Experimental (a) and theoretical (b) Raman spectra of 2-aminobenzimidazole.

literature data (1.389–1.413 Å) [18]. Both the N–H bond lengths in amino group are same in B3LYP/6-311++G(d,p) method, i.e., 1.011 Å. With the electron donating substituents on the benzene ring, the symmetry of the ring is distorted, yielding ring angles smaller than 120° at the point of substitution and slightly larger than 120° at the ortho and meta positions [34]. Thus, in 2-ABD molecule the bond angles C3–C4–C5, C2–C1–C5 are larger than 120° while at substitution position, the angle N8–C14–N9 is found to be less than 120°, respectively.

5.2. Vibrational assignments

The main objective of the vibrational analysis is to find vibrational modes connected with specific molecular structures of calculated compound. In order to get the best possible fitting between the calculated and experimental vibrational wavenumbers the scaled quantum mechanic force field (SQMFF) was applied. The title molecule consists of 17 atoms, hence undergoes 45 normal modes of vibrations. The molecule under investigation possess C_1 point group symmetry. The atomic displacements corresponding to the different normal modes are identified using Gauss view program package [35]. The observed and calculated wavenumbers along with relative intensities, probable assignments and total energy distribution (TED) are presented in Table 3. The experimental IR-LD spectral data of protonated salt of 2-aminobenzimidazole taken from Ref. [17] are also reported in Table 3 and are compared with our experimental FTIR, FT-Raman and theoretical data. The experimental and theoretical FTIR and FT-Raman spectra are shown in Figs. 2 and 3. Calculated Raman and IR intensities help us to distinguish and more precisely assign those fundamentals which are close in frequency. Although basis sets are marginally sensitive as observed in the DFT values using 6-311++G (d,p), reduction in the computed harmonic vibrational wavenumbers is noted. In our present investigation, wavenumbers in the ranges from 4000 to 1700 cm^{-1} and lower than 1700 cm^{-1} are scaled with 0.958 and 0.983, respectively [36]. The scale factor of 0.9613 is used for B3LYP/6-31G(d) method in the present work. The scaled wavenumbers minimize the root-mean square difference between calculated and experimental wavenumbers for bands with definite identifications.

5.2.1. C–H vibrations

The assignments of carbon–hydrogen stretching modes are straight forward on the basis of the scaled ab initio predicted frequencies as well known "group frequencies". For simplicity, modes of vibrations of aromatic compounds are considered as separate C–H or ring C–C vibrations. However, as with any complex molecules, vibrational interactions occur and these labels only indicate the predominant vibration. Usually the carbon hydrogen stretching vibrations give rise to bands in the region of 3100–3000 cm^{-1} in all aromatic compounds [37,38]. In this region, the bands are not affected appreciably by the nature of the substituents. All the aromatic C–H stretching bands are found to be weak and this is due to decrease of dipole moment caused by reduction of the negative charge on the carbon atom. This reduction occurs because of the electron withdrawal on the carbon atom by substituent due to the decrease of inductive effect, which in turn by the increase in chain length of the substituent [39]. The 2-ABD has four C–H moieties correspond to aromatic ring stretching vibrations as shown in Fig. 1. The expected four C–H stretching vibrations of the 2-ABD corresponds to (mode nos. 4–7) stretching modes of C3–H, C4–H, C5–H and C10–H units. The C–H stretching vibration is observed in FTIR spectrum at 3079, 3065 and 3054 cm^{-1} and in FT-Raman spectrum at 3067 and 3057 cm^{-1}. The similar vibration is calculated at 3061, 3052, 3040 and 3032 cm^{-1} by B3LYP/6-311++G(d,p) method and at 3091, 3081, 3069 and 3060 cm^{-1} by B3LYP/6-31G(d) method and it shows very good correlation with the experimental data. The total energy distribution contribution of 100% of these aromatic stretching modes indicates that these are highly pure stretching modes and are indicated in Table 3.

The in-plane C–H bending vibrations appear in the range of 1300–1000 cm^{-1} in the substituted benzenes and the out-of-plane bending vibrations occur in the frequency range of 1000–750 cm^{-1} [40,41]. The C–H in-plane bending vibrations of benzimidazole are coupled with ring C–C and C=N stretching modes as evident from TED. The C–H in-plane and out-of-plane bending vibrations are computed theoretically at 1233, 1153, 1111 cm^{-1} and 953, 914, 836, 747 cm^{-1} by B3LYP/6-311++G(d,p) method respectively. IR active C–H in plane bending vibration of title molecule appears at 1245, 1158 and 1108 cm^{-1} with maximum TED contribution of 79%. The Raman active bands at 1253, 1160 and 1109 cm^{-1} are corresponding to the C–H in-plane bending modes. The corresponding C–H out-of-plane bending vibrations are observed in FTIR at 917 and 757 cm^{-1} in IR-LD at 917 cm^{-1} [17] and in FT-Raman at 755 cm^{-1} and are in agreement with the theoretical values.

5.2.2. Amino group vibrations

The fundamental modes involving the amino group are stretching and bending of NH band, torsion and inversion. It is stated that in amines, the N–H stretching vibrations occur in the region of 3500–3300 cm^{-1} [42]. The NH_2 group has two vibrations; one is being asymmetric and other symmetric. The frequency of asymmetric vibration is higher than that of symmetric one.

Table 3
Comparison of the calculated and experimental vibrational spectra and proposed assignments of 2-aminobenzimidazole.

Mode nos.	Experimental wavenumbers (cm^{-1})			Theoretical wavenumbers (cm^{-1})						TED (≥10%)
	FT-IR	FT-Raman	IR-LD 2-ABD[a]	B3LYP/6-311++G(d,p)			B3LYP/6-31G(d)			
				Scaled	I_{IR}	I_{Ra}	Scaled	I_{IR}	I_{Ra}	
1				3501	51.09	0.04	3508	42.15	111.21	υ N9H (100)
2	3390			3499	37.17	0.03	3491	25.23	93.44	υ_{asym} NH_2 (100)
3	3376		3376	3405	34.18	0.11	3392	18.57	292.62	υ_{sym} NH_2 (100)
4	3079			3061	10.31	0.15	3091	15.57	218.28	υ CH (97)
5	3065	3067		3052	20.17	0.06	3081	30.70	119.86	υ CH (100)
6	3054	3057		3040	12.34	0.07	3069	16.94	114.36	υ CH (99)
7				3032	0.06	0.03	3060	0.03	48.36	υ CH (100)
8	1667	1666	1666	1652	214.48	0.11	1637	190.08	24.48	υ CC (23) + ρ NH_2 (18) + υ C14N8 (17)
9	1622	1622	1623	1621	75.35	0.31	1610	36.12	46.42	ρ NH_2 (45) + υ CC (24)
10	1595	1597		1596	19.46	0.03	1579	8.13	6.43	υ CC (64)
11	1564		1565	1561	188.89	0.48	1545	187.80	64.06	υ C14N8 (25) + ρ NH_2 (24) + υ C14N15 (12)
12	1481			1490	8.51	0.02	1475	7.43	3.38	υ CC (28) + β CH (25) + υ_{asym} C14N8N9 (11)
13	1463	1464		1457	61.75	0.13	1444	40.73	11.89	β CH (42) + υ CC (26)
14	1456			1450	127.72	0.07	1437	136.07	11.16	υ_{asym} C14N8N9 (35) + r NH_2 (20)
15	1380	1385		1378	0.74	0.08	1365	1.07	8.57	υ CC (41) + β CH (18)
16	1313	1317		1313	4.72	0.04	1297	1.73	2.18	υ CC (57)
17	1270	1271	1270	1262	73.06	1.00	1251	70.43	83.73	υ CC (45) + υ CN (36)
18	1245	1253		1233	14.21	0.32	1216	8.31	18.07	β CH (28) + β N9H (23) + υ CC (12) + υ C2N8 (10)
19	1214			1201	2.21	0.01	1185	0.68	0.64	υ CN (28) + β N9H (21) + β CCC (17)
20	1158	1160		1153	2.04	0.07	1138	1.36	4.07	β CH (79) + υ CC (12)
21	1108	1109		1111	0.49	0.14	1100	4.25	14.26	β CH (42) + υ CC (29)
22				1103	12.63	0.05	1093	9.10	1.67	r NH_2 (51) + υ C14N8 (14)
23	1035	1036		1014	7.86	0.56	1002	3.84	22.69	υ CC (70)
24	1003	1006		993	3.75	0.00	980	2.96	0.84	υ C14N9 (49) + υ CC (16)
25				953	0.13	0.00	928	0.09	0.29	γ CH (89)
26	917		917	914	3.36	0.00	883	2.43	0.88	γ CH (91)
27	898	873		890	3.09	0.03	871	3.77	0.81	β CCC (54) + υ CN (17)
28	849	850		843	0.87	0.44	829	3.45	11.46	υ CC (38) + υ CN (11) + β NCN (10)
29				836	0.71	0.03	824	0.69	5.75	γ CH (86)
30	757	755		747	33.25	0.03	750	236.80	7.45	γ CCC (60) + γ CH (14)
31	742			736	101.03	0.09	736	26.79	1.65	γ CCC (32) + ω NH_2 (19) + γ CCC (19)
32	729		728	724	26.50	0.05	722	27.73	3.34	γ CCC (39) + γ NCN (37)
33	692	692		688	5.63	0.66	673	3.73	11.41	γ CCC (19) + γ CNC (14) + υ C-NH_2 (14)
34	625	625		632	233.60	0.28	644	165.11	2.90	ω NH_2 (62)
35				619	24.26	0.36	606	3.60	6.92	γ CCC (40) + γ NCC (22) + υ CC (16)
36	581			576	9.17	0.03	565	4.58	0.20	γ CCC (61) + γ CNC (15)
37	503	507		502	2.55	0.15	491	0.63	7.52	r NH_2 (29) + β CCN (21) + γ CCC (15)
38	491		480	499	10.05	0.93	487	12.91	3.83	β CCC (26) + β CCN (14) + β N–C–NH_2 (14) + υ CN (12)
39	433			431	13.70	0.05	427	9.41	0.45	γ CCC (71)
40		347		376	68.55	0.32	368	89.32	2.32	γ N9H (85)
41		323		329	16.64	0.20	326	25.60	3.08	γ CNC (72)
42				286	10.64	0.01	286	53.42	2.48	β NCN15 (40) + β CCN (17)
43		261		277	62.58	0.00	275	18.24	0.85	τ NH2 (78)
44				240	8.55	0.00	239	7.41	0.60	γ CCN (50) + γ CCC (25)
45		103		138	9.98	0.00	137	9.41	0.72	butterfly (86)
RMS				12.7189			19.49			

[a] Taken from Ref. [17]. IR-LD, infrared linear dichroic; 2-ABD, 2-aminobenzimidazole; I_{IR}, IR intensity (Km mol^{-1}); I_{Ra}, Raman intensity (Arb. units) (relative Raman intensities and normalized to 1); ν, stretching; β, in-plane-bending; γ, out-of-plane bending; ρ, scissoring; ω, wagging; r, rocking; τ, torsion.

Table 4
The observed and computed absorption wavelength λ (nm), excitation energies E (eV), absorbance and oscillator strengths f (a.u.) of 2-ABD in gas phase, ethanol and water, $CDCl_3$ and DMSO solutions.

Experimental			TD-DFT/B3LYP/6-311++G(d,p)															
Ethanol			Water			Gas			Ethanol			Water			$CDCl_3$			DMSO		
λ (nm)	E (eV)	Abs.	λ (nm)	E (eV)	Abs.	λ (nm)	E (eV)	f (a.u.)	λ (nm)	E (eV)	f (a.u.)	λ (nm)	E (eV)	f (a.u.)	λ (nm)	E (eV)	f (a.u.)	λ (nm)	E (eV)	f (a.u.)
283	4.39	0.407	280	4.43	0.277	279	4.44	0.0050	259	4.79	0.1856	259	4.79	0.1818	259	4.79	0.1956	259	4.79	0.2430
243	5.11	0.299	244	5.09	0.141	256	4.84	0.1071	247	5.02	0.0024	246	5.04	0.0022	254	4.89	0.0028	241	5.14	0.0706
212	5.86	1.798	204	6.08	1.643	235	5.01	0.0119	239	5.20	0.0819	239	5.20	0.0790	239	5.19	0.0959	236	5.26	0.0008

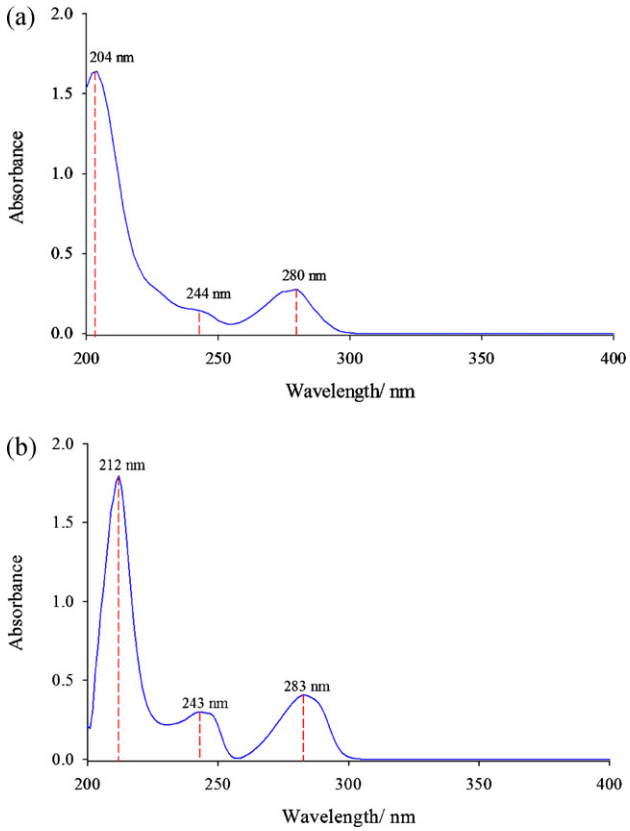

Fig. 4. Experimental UV spectra of 2-aminobenzimidazole (a) in water and (b) in ethanol.

The asymmetric $-NH_2$ stretching vibration appears from 3500 to 3420 cm^{-1} and the symmetric $-NH_2$ stretching vibration is observed in the range of 3420–3340 cm^{-1}. Based on the above conclusion in our present study, the strong band observed in FTIR spectrum at 3390 cm^{-1} is assigned to NH_2 asymmetric stretching and 3376 cm^{-1} is assigned to NH_2 symmetric stretching vibrations. There is no peaks observed for NH_2 stretching vibrations in FT-Raman spectrum. The NH_2 asymmetric and symmetric stretching vibrations are computed theoretically by B3LYP/6-311++G(d,p) method at 3499 and 3405 cm^{-1} and by B3LYP/6-31G(d) method at 3491 and 3392 cm^{-1} (mode nos. 2 and 3). The calculated values are in line with the experimental values and literature data of 3376 cm^{-1} [17]. As evident from Table 3, the TED of these modes are exactly contributing to 100%.

Bellamy [40] and Mancy et al. [43] suggested that the NH_2 scissoring mode lies in the region of 1529–1650 cm^{-1}. In accordance with above conclusion in our present study the NH_2 scissoring mode computed at 1652, 1621 and 1561 cm^{-1} (B3LYP/6-311++G(d,p)) and at 1637, 1610 and 1545 cm^{-1} (B3LYP/6-31G(d)) (mode nos. 8, 9 and 11) show good agreement with recorded FTIR bands at 1667, 1622, 1564 cm^{-1} and 1666, 1622 cm^{-1} in

Table 5
Calculated energies values of 2-aminobenzimidazole for ground state in gas phase, $CDCl_3$ and DMSO solutions.

TD-DFT/B3LYP/6-311++G(d,p)	Gas	$CDCl_3$	DMSO
E_{total} (Hartree)	−435.3511	−435.3612	−435.3390
E_{HOMO} (eV)	−0.21450	−0.21894	−0.22956
E_{LUMO} (eV)	−0.02524	−0.02028	−0.03448
$\Delta E_{HOMO-LUMO\ gap}$ (eV)	−0.18926	−0.19866	−0.19508
E_{HOMO-1} (eV)	−0.23320	−0.23804	−0.24499
E_{LUMO+1} (eV)	−0.01527	−0.01202	−0.00916
$\Delta E_{HOMO-1-LUMO+1\ gap}$ (eV)	−0.21793	−0.22602	−0.23583

FT-Raman and also show good agreement with literature data of 1666 and 1623 cm^{-1} [17]. The NH_2 wagging vibration analogous to the inversion mode of ammonia is so strongly anharmonic that it cannot be reproduced by the harmonic treatment [44]. The NH_2 wagging mode for 2-ABD is observed as a medium band in FTIR spectrum at 742 and 625 cm^{-1} and in FT-Raman spectrum at 625 cm^{-1} and it shows better agreement with the predicted value of 736 and 632 cm^{-1} (mode nos. 31 and 34) by B3LYP/6-311++G(d,p) method. The NH_2 twisting wavenumber is expected to occur in the region of 1060–1170 cm^{-1}. The NH_2 twisting mode for 2-ABD is calculated at 1103 cm^{-1} (mode no. 22). The TED contribution of this mode is 51% mixed with minor contribution of 14% of νCN. The NH_2 torsion can be expected in the low wavenumber range, the wavenumber computed and assigned by Gauss view animation package at 277 cm^{-1} (mode no. 43) is assigned to NH_2 torsional vibration of 2-ABD and it shows satisfactory agreement with recorded FT-Raman wavenumber at 261 cm^{-1} and also show deviations of about 16 cm^{-1}. As indicated by the TED, this mode involves maximum contribution of 78% suggesting that this is a pure mode. The N–H vibrations of present molecule affect the other vibrational modes whereas the N–H vibrations themselves do not get affected by vibrations of other substitutions.

5.2.3. N–H vibrations

It has been observed that the presence of N–H group in various molecules may be correlated with a constant occurrence of absorption bands whose positions are slightly altered from one compound to another, this is because the atomic group vibrates independently of the other groups in the molecule and has its own frequency. The position of absorption in this region depends upon the degree of hydrogen bonding, and hence upon the physical state of the sample. The spectral lines assigned to N–H stretching vibrations have shifted to higher region in the present system. It clearly indicates that the stretching of N–H bond upon protonation has shifted the frequency to a higher region. Another possible cause for the stretching may be due to the occurrence of N–H and C–H hydrogen bonds in the atomic sites of the benzene and imidazole rings (CH···NH = 2.912 Å). Normally in all the heterocyclic compounds, the N–H stretching vibration occurs in the region of 3500–3000 cm^{-1} [38]. The N–H stretching was assigned to the band at 3460 cm^{-1} in the case of benzimidazole [18]. In our title molecule, the N–H stretching vibration is predicted at 3501 cm^{-1} by B3LYP/6-311++G(d,p) and at 3508 cm^{-1} by B3LYP/6-31G(d) method. This mode is pure stretching mode as it is evident from Table 3, which is exactly contributing to 100% of TED. This predicted wavenumber is exactly correlated with the literature data [19].

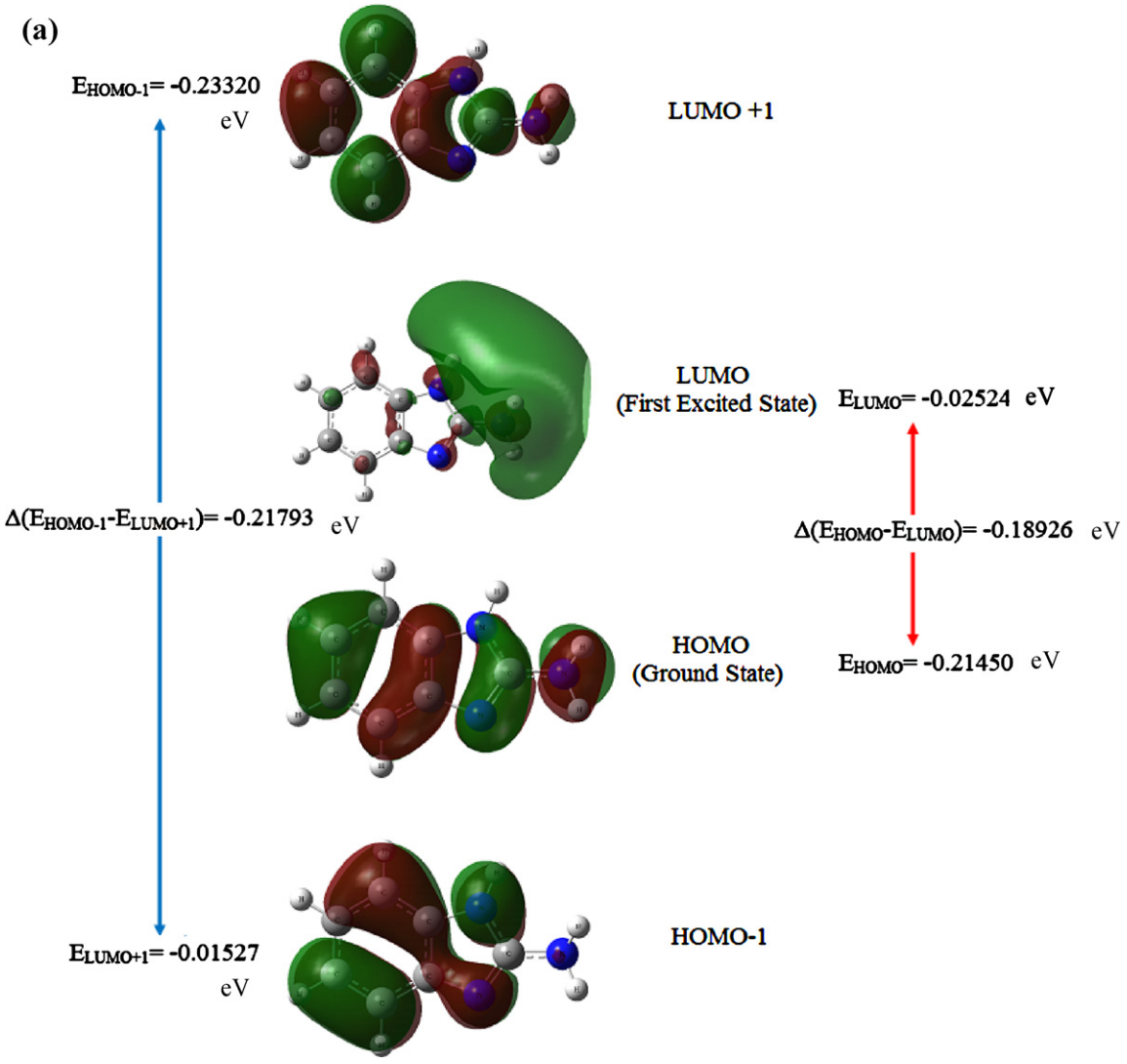

Fig. 5. The atomic orbital compositions of the frontier molecular orbital for 2-aminobenzimidazole in (a) gas phase. The atomic orbital compositions of the frontier molecular orbital for 2-aminobenzimidazole in (b) chloroform. The atomic orbital compositions of the frontier molecular orbital for 2-aminobenzimidazole in (c) DMSO solution.

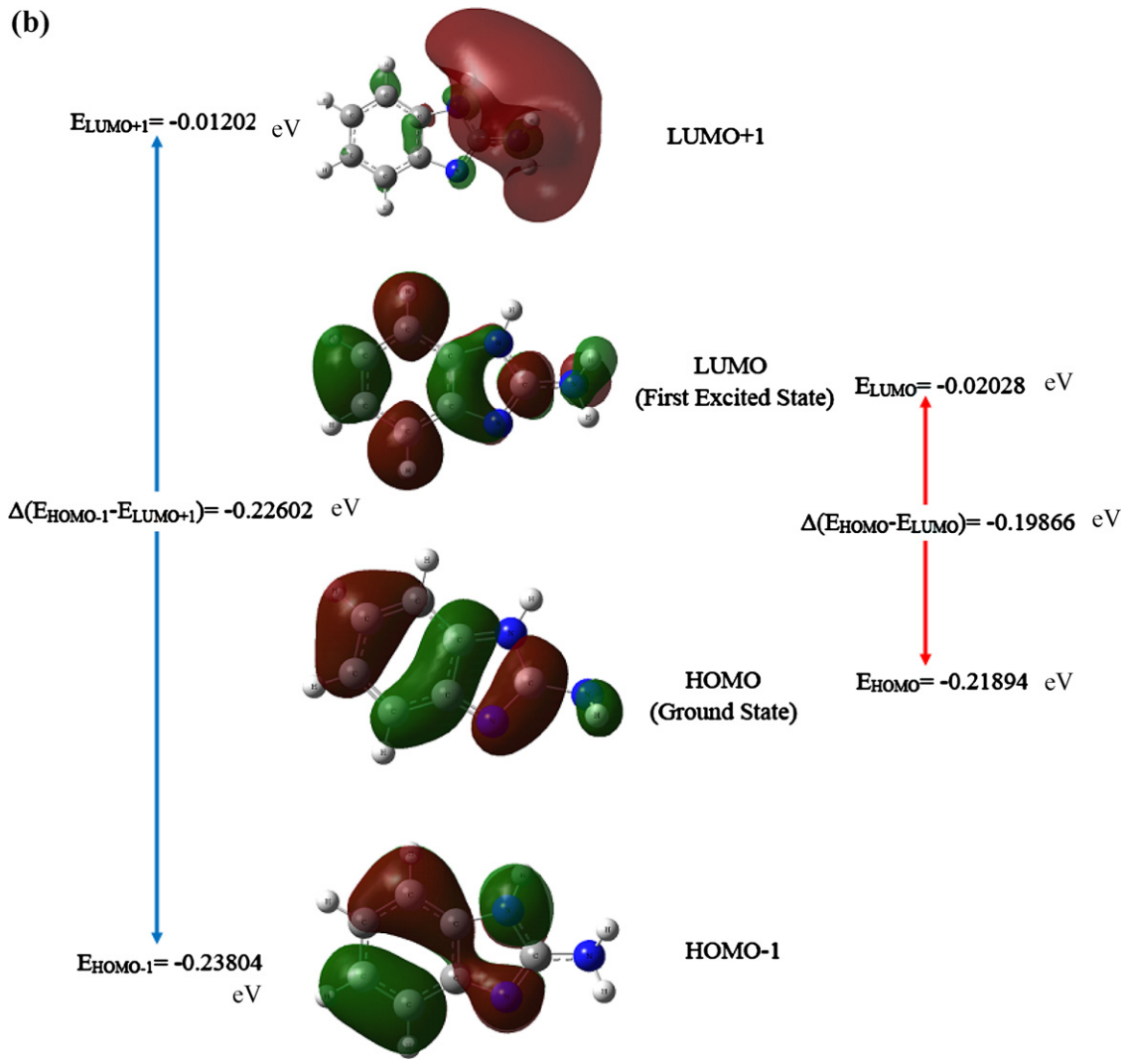

Fig. 5. (*Continued*).

There are no peaks observed in both FTIR and FT-Raman spectra for N–H stretching vibration. The N–H in-plane and out-of-plane bending vibrations are assigned to the wavenumbers at 1233, 1201 cm^{-1} and 376 cm^{-1} respectively, predicted by B3LYP/6-311++G(d,p) for 2-ABD. These calculated wavenumbers are consistent with the observed wavenumbers and the literature data.

5.2.4. Ring vibrations

The aromatic ring vibrational modes of title compound have been analyzed based on the vibrational spectra of previously published vibrations of the benzene molecule are helpful in the identification of the phenyl ring modes [45,46]. The ring stretching vibrations are very prominent, as the double bond is in conjugation with the ring, in the vibrational spectra of benzene and its derivatives [47]. The ring carbon–carbon stretching vibration occurs in the region of 1650–1200 cm^{-1}. In general, the bands are of variable intensity and are observed at 1625–1590, 1590–1575, 1540–1470, 1430–1465 and 1380–1280 cm^{-1} from the frequency ranges given by Varsanyi [48] for the five bands in the region. In the present study, the wavenumbers observed in the FTIR spectrum at 1667, 1622, 1595, 1481, 1463, 1380, 1313 and 1270 cm^{-1} are assigned to C–C stretching vibrations. The same vibrations appear in the FT-Raman spectrum at 1666, 1622, 1597, 1464, 1385, 1317 and 1271 cm^{-1}. The computed wavenumber for C–C stretching vibrations are found in the range of 1652–1262 cm^{-1} (mode nos. 8–10, 12, 13 and 15–17) by B3LYP/6-311G++(d,p) and in the range of 1637–1251 cm^{-1} by B3LYP/6-31G(d) method. The observed values are in good correlation with the literature data of 1666, 1623 and 1270 cm^{-1} [17] and calculated values. The TED corresponding to these vibrations are mixed mode of contributing less than 50%. The in-plane deformation vibrations are at higher wavenumbers than out-of-plane vibrations. Shimanouchi et al. [49] gave the frequency data for these vibrations for different benzene derivatives as a result of normal coordinate analysis. For aromatic ring, some bands are observed below 700 cm^{-1}, these bands are quite sensitive to change in the nature and position of the substituents [50–53]. Although other bands depend mainly on the substitution and the number of substituent rather than on their chemical nature or mass, so that these latter vibrations, together with the out-of-plane vibrations of the ring hydrogen atoms are extremely useful in determining the positions of substituents. The band occurring at 898 cm^{-1} in the infrared and at 873 cm^{-1} in Raman spectrum is assigned to the CCC in-plane bending modes of 2-ABD. The predicted wavenumber of 890 cm^{-1} is well correlated with the experimental wavenumber. The theoretically computed wavenumbers of CCC out-of-plane bending vibrations are also in good agreement with the measured values and literature data [17].

The identifications of C=N and C–N vibrations is a difficult task, since the mixing of several bands are possible in the region.

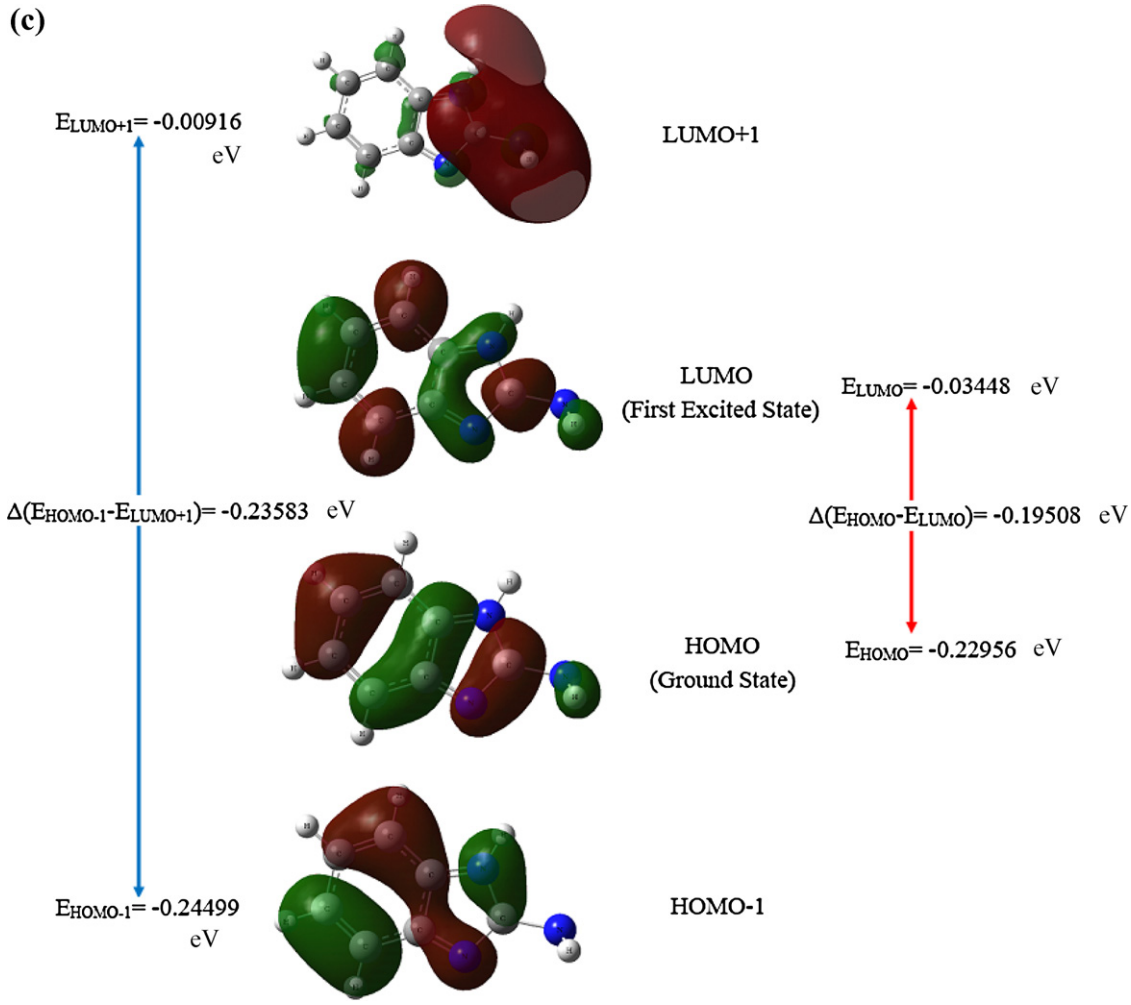

Fig. 5. (*Continued*).

Silverstein et al. [41] assigned C=N stretching absorption in the region of 1382–1266 cm^{-1} for aromatic amines. In benzamide the band observed at 1368 cm^{-1} is assigned to C=N stretching [54]. Sundaraganesan et al. [18] assigned C–N stretching vibration at 1281 cm^{-1} for benzimidazole. In the present work, the FTIR bands observed at 1456 and 1270 cm^{-1} and FT-Raman band at 1271 cm^{-1} have been assigned to C–N stretching vibrations and the band at 1564 cm^{-1} in FTIR and the band at 1565 cm^{-1} in IR-LD is assigned to C=N stretching vibration of 2-ABD. The predicted value of C=N stretching vibration is 1561 cm^{-1} and C–N stretching vibrations are 1450 and 1262 cm^{-1} (mode nos. 11, 14 and 17). In addition to these vibrations, the C–N–C, N–C–N, C–C–N bending vibrations (i.e. in-plane and out-of-plane) have been assigned by TED shows good agreement with recorded spectral data. The ring butterfly mode is calculated at 138 cm^{-1} by B3LYP/6-311++G(d,p) method and at 137 cm^{-1} by B3LYP/6-31G(d) method and the TED contribution of this mode is 86%.

In order to investigate the performance and vibrational wavenumbers for the title compound, root mean square (RMS) value for each basis set was also calculated and are given in Table 3. The RMS values were obtained in this study using the following expression [55]:

$$\mathrm{RMS} = \sqrt{\frac{1}{n-1}\sum_{i}^{n}(\nu_i^{calc} - \nu_i^{exp})^2}$$

The RMS error of the calculated bands are found to be 12.7189 and 19.49 for B3LYP/6-311++G(d,p) and B3LYP/6-31G(d) methods respectively.

5.3. UV–VIS spectral analysis

Ultraviolet spectra analysis of 2-aminobenzimidazole have been investigated in the gas phase and in two different solvents (ethanol and water) by theoretical calculation. On the basis of fully optimized ground-state structure, TD-DFT/B3LYP/6-311++G(d,p) calculations have been used to determine the low-lying excited states of 2-ABD. The calculated visible absorption maxima of λ which are a function of the electron availability have been reported in Table 4. The experimental UV spectra of 2-ABD are shown in Fig. 4. The theoretical electronic excitation energies, oscillator strengths, absorption wavelength and nature of the first 10 spin-allowed singlet–singlet excitations were also calculated by the TD-DFT method for the same solvents and are also listed in Table 4. Calculations of the molecular orbital geometry show that the visible absorption maxima of this molecule correspond to the electron transition between frontier orbitals such as translation from HOMO to LUMO. As can be seen from Table 4, the calculated absorption maxima values have been found to be 279, 256 and 235 nm for gas phase, 259, 247 and 239 nm for ethanol solution and 259, 246 and 239 nm for water at DFT/B3LYP/6-311++G(d,p) method. The measured absorption maxima values have been found to be 283, 243 and 212 nm for ethanol and 280, 244 and 204 nm for water. It is

seen from Table 4, calculations performed at ethanol solution and water are close to each other when compared with gas phase and also the absorption maxima values of gas phase are larger than that of the organic solvents.

5.4. Frontier molecular orbital analysis

Molecular orbitals (HOMO and LUMO) and their properties such as energy are very useful for physicists and chemists and are very important parameters for quantum chemistry. This is also used by the frontier electron density for predicting the most reactive position in π-electron systems and also explains several types of reaction in conjugated system [56]. Both the highest occupied molecular orbital (HOMO) and lowest unoccupied molecular orbital (LUMO) are the main orbital take part in chemical stability [57]. The energies of four important molecular orbitals of 2-ABD: the second highest and highest occupied MO's (HOMO and HOMO−1), the lowest and the second lowest unoccupied MO's (LUMO and LUMO+1) are calculated in gas phase $CDCl_3$ and DMSO solutions and are presented in Table 5.

The HOMO represents the ability to donate an electron, LUMO as an electron acceptor represents the ability to obtain an electron. The energy gap between HOMO and LUMO is a critical parameter in determining molecular electrical transport properties [58]. The energy gap between HOMO and LUMO explains the biological activity [59] of the molecule, which is due to the change in partial charge and to the change in total dipole moment [60,61]. The plots of highest occupied molecular orbitals (HOMOs) and lowest unoccupied molecular orbitals (LUMOs) are shown in Fig. 5. This electronic absorption corresponds to the transition from the ground to the first excited state and is mainly described by one electron excitation from the highest occupied molecular orbital (HOMO) to the lowest unoccupied molecular orbital (LUMO). While the energy of the HOMO is directly related to the ionization potential, LUMO energy is directly related to the electron affinity.

The HOMO is located over the benzimidazole ring, the HOMO → LUMO transition implies an electron density transfer to amino group from benzimidazole ring. Moreover, these orbital significantly overlap in their position for 2-ABD and lower in the HOMO and LUMO energy gap explains the eventual charge transfer interactions taking place within the molecule.

The HOMO and LUMO energy calculated by B3LYP/6-311++G(d,p) method in gas phase is given below.

HOMO energy (B3LYP) = −0.2145 eV

LUMO energy (B3LYP) = −0.0252 eV

HOMO–LUMO energy gap (B3LYP) = −0.1893 eV

6. Conclusion

The detailed interpretation of the vibrational spectra has been carried out with the aid of scaled quantum mechanical method. FTIR and FT-Raman spectra of 2-aminobenzimidazole have been recorded and analyzed. The molecular geometry, vibrational wavenumbers, UV–Vis analysis, HOMO and LUMO energy of 2-aminobenzimidazole in the ground state have been calculated by using density functional theory. The observed and the calculated wavenumbers are found to be in good agreement with majority modes. The lowering of the HOMO–LUMO energy gap value has substantial influence on the intramolecular charge transfer and bioactivity of the molecule. The UV spectra were measured in ethanol solution and water and the results are compared with the theoretical results.

References

[1] The Merck Index, An Encyclopedia of Chemical Drugs and Biologicals, 12th edition, Merck and Co., Whitehouse Station, NY, USA, 1996.
[2] W. Nawrocka, M. Zimecki, T. Kuznicki, M.W. Kowalska, Arch. Pharm. 332 (1999) 85.
[3] H. Wahe, P.F. Asobo, R.A. Cherkasov, A.E. Nkengfack, G.N. Folefoc, Z.T. Fomum, D. Doepp, Arkivoc (2003) 170.
[4] M. Cuberens, M.R. Contijoch, Chem. Pharm. Bull. 45 (1997) 1287.
[5] M. Mor, F. Bordi, C. Silva, S. Rivara, V. Zuliani, F. Vacondio, Bioorg. Med. Chem. 12 (2004) 663.
[6] A.D. Dios, C. Shih, B.L. de Uralde, C. Sanchez, M. Del Prado, L.M.M. Cabrejas, S. Pleite, J. Med. Chem. 48 (2005) 2270.
[7] L.B. Townsed, J. Drach, Polysubstituted benzimidazoles as antiviral agents, US 5,574,058 C.A. 126 60293c, 1997.
[8] S.D. Chamberlein, G.W. Koszalka, Preparation of benzimidazole containing nucleofile analogs as virucides, WO 96, 01,833 C.A. 124 317788w; 1996.
[9] E.A.M. Badaway, T. Kappe, Arch. Pharm. Pharm. Med. Chem. 330 (1997) 59.
[10] I. Iriepa, B. Gil-Alberdi, E. Gálvez, F.J. Villasante, J. Bellanato, P. Carmona, J. Mol. Struct. 482 (1999) 437.
[11] M.G. Vigorita, T. Previtera, C. Zappalà, A. Trovato, M.T. Monforte, R. Barbera, F. Pizzimenti, Farmaco Societa Chimica Italiana 45 (1990) 223.
[12] W. Nawrocka, Boll. Chim. Farm. 135 (1996) 18.
[13] S.S. Kukalenko, V.A. Udovenko, V.P. Borysova, N.L. Kulugina, N.M. Burmakin, E.L. Andreeva, U.S.S.R. SU 1,636,414, Odkrytiya Izobret 11 (1991) 75.
[14] F. Esser, G. Schonnenberg, H. Dollinger, W. Geida, Ger. Offen DE (1999) 19.816,915 (Cl C07k5/06), C.A. 131 P 272188 a.
[15] D. Nikolova, R. Ivanov, S. Buyukliev, M. Konstantinov, M. Karaivanova, Arzneim-Forsch. Drug Res. 51 (2001) 758.
[16] D. Jornet, P. Bartovsky, L.R. Domingo, R. Tormos, M.A. Miranda, J. Phys. Chem. 114B (2010) 11920.
[17] B.B. Ivanova, Spectrochim. Acta 62A (2005) 58.
[18] N. Sundaraganesan, S. Ilakiamani, P. Subramani, B.D. Joshua, Spectrochim. Acta 67A (2007) 628.
[19] M.T. Güllüoglu, M. Özduran, M. Kurt, S. Kalaichelvan, N. Sundaraganesan, Spectrochim. Acta 76A (2010) 107.
[20] M.T. Güllüoğlu, Y. Erdogdu, J. Karpagam, N. Sundaraganesan, Ş. Yurdakul, J. Mol. Struct. 990 (2011) 14.
[21] S.E. Angelova, M.I. Spassova, V.V. Deneva, M.I. Rogojerov, L.M. Antonov, ChemPhysChem 12 (2011) 1747.
[22] J.B. Foresman, A. Frisch, Exploring Chemistry with Electronic Chemical Structure Methods, 2nd edition, Gaussian Inc., Pittsburg, PA, 1996.
[23] K. Golcuk, A. Altun, M. Kumru, Spectrochim. Acta 59A (2003) 1841.
[24] C. Ravikumar, I.H. Joe, V.S. Jayakumar, Chem. Phys. Lett. 460 (2008) 552.
[25] Gaussian Inc., Gaussian 03 Program, Gaussian Inc., Wallingford, 2004.
[26] M.H. Jamróz, Vibrational energy distribution analysis, VEDA 4 Computer Program, Poland, 2004.
[27] G. Keresztury, S. Holly, J. Varga, G. Besenyei, A.Y. Wang, J.R. Durig, Spectrochim. Acta 49A (1993) 2007.
[28] G. Keresztury, Raman spectroscopy: theory, in: J.M. Chalmers, P.R. Griffith (Eds.), Hand Book of Vibrational Spectroscopy, vol. 1, John Wiley & Sons Ltd, New York, 2002.
[29] D.A. Kleinman, Phys. Rev. 126 (1962) 1977.
[30] C.J. Dik-Edixhoven, H. Schent, H. Van der Meer, Cryst. Struct. Commun. 2 (1973) 1647.
[31] J.V. Prasad, S.B. Rai, S.N. Thakur, Chem. Phys. Lett. 164 (1989) 629.
[32] M.K. Ahmed, B.R. Henry, J. Phys. Chem. 90 (1986) 629.
[33] R.I. Castillo, L.A. Rivera-Montalvo, S.P. Hernandez-Rivera, J. Mol. Struct. 877 (2008) 10.
[34] Y. Wang, S. Saebar, C.U. Pittman, J. Mol. Struct.: Theochem. 281 (1993), 9l.
[35] R. Dennington II, T. Keith, J. Millam, GaussView, Version 4.1.2, Semichem Inc., Shawnee Mission, KS, 2007.
[36] N. Sundaraganesan, S. Illakiamani, H. Saleem, P.M. Wojciechowski, D. Michalska, Spectrochim. Acta 61A (2005) 2995.
[37] R.L. Peesole, L.D. Shield, I.C. McWillam, Modern Methods of Chemical Analysis, Wiley, New York, 1976.
[38] G. Socrates, Infrared and Raman Characteristic Group Frequencies – Tables and Charts, third edition, Wiley, Chichester, 2001.
[39] N. Sundaraganesan, H. Saleem, S. Mohan, Spectrochim. Acta 59A (2003) 2511.
[40] V. Krishnakumar, S. Dheivamalar, Spectrochim. Acta 71A (2008) 465.
[41] M. Silverstein, G. Clayton Basseler, C. Morill, Spectrometric Identification of Organic Compounds, Wiley, New York, 1981.
[42] L.J. Bellamy, The Infrared Spectra of Complex Molecules, vol. 2, Chapman and Hall, London, 1980.
[43] S. Mancy, W.L. Peticoles, R.S. Toblas, Spectrochim. Acta 35A (1979) 315.
[44] P.M. Wojciechawski, W. Zierkiewicz, D. Michalska, P. Hobza, J. Chem. Phys. 118 (2003) 1090.
[45] N.B. Colthup, L.H. Daly, S.E. Wiberley, Introduction to Infrared and Raman Spectroscopy, Academic Press, New York, 1990.
[46] G. Socrates, Infrared Characteristic Group Frequencies, Wiley Interscience Publication, 1980.
[47] G. Varsanyi, Vibrational Spectra of Benzene Derivatives, Academic Press, New York, 1969.
[48] G. Varsanyi, Assignments of Vibrational Spectra of Seven Hundred Benzene Derivatives, vols. 1–2, Adam Hilger, 1974.
[49] T. Shimanouchi, Y. Kakiuti, I.J. Gamo, Chem. Phys. 25 (1956) 1245.

[50] R.J. Jakobsen, F.F. Bentely, Appl. Spectrosc. 18 (1964) 88.
[51] A.J. Mansingh, Chem. Phys. 52 (1970) 5896.
[52] L. Verdonok, G.P. Van Der Kelen, Z. Eeckhant, Spectrochim. Acta 28A (1972) 51.
[53] A.P. Datin, J.M. Lebas, Spectrochim. Acta 25A (1969) 168.
[54] R. Shanmugam, D. Sathyanarayanan, Spectrochim. Acta 40A (1984) 757.
[55] V. Krishnakumar, S. Dheivamalar, R. John Xavier, V. Balachandran, Spectrochim. Acta 65A (2006) 147.
[56] K. Fukui, T. Yonezawa, H. Shingu, J. Chem. Phys. 20 (1952) 722.
[57] S. Gunasekaran, R.A. Balaji, S. Kumeresan, G. Anand, S. Srinivasan, Can. J. Anal. Sci. Spectrosc. 53 (2008) 149.
[58] K. Fukui, Science 218 (1982) 747.
[59] D. Sajan, K.U. Lakshmi, Y. Erdogdu, I.H. Joe, Spectrochim. Acta 78A (2011) 113.
[60] M. Ibrahim, A.A. Mahmoud, J. Comput. Theor. Nanosci. 6 (2009) 1523.
[61] M. Ibrahim, H. El-Haes, Int. J. Environ. Pollut. 23 (2005) 417.